3-D common-azimuth wave-equation migration velocity analysis

Weihong Fei[1], Paul Williamson[1], and Alexandre Khoury[2]*
[1] Total E&P USA, [2]Total-CSTJF, Pau, France

Summary

We present a 3-D automatic migration velocity analysis (MVA) algorithm based on common-azimuth migration (CAM) in the source-geophone implementation, and using differential semblance optimization (DSO). We have successfully tested the algorithm on the 3-D SEG/EAGE overthrust model and a 3D field dataset using a simple 1D velocity model as a starting point in each case. We conclude that wave-equation-based MVA may be a good alternative to ray-based tomography for velocity model-building in complex regions of the earth.

Introduction

An accurate velocity model is a prerequisite for satisfactory depth migration. Although ray-based tomography (e.g. Bishop et al., 1985, Sexton and Williamson, 1998) is still the workhorse for velocity model-building in the industry, interest has been growing in band-limited methods which more accurately represent the underlying physics, such as one-way wave equation-based MVA (Sava and Biondi, 2004; Shen et at 2003; Xie and Yang 2008; Fliedner et al, 2007; Albertin et al, 2006), and full waveform inversion (Tarantola, 1984: Pratt, 1999; Hadj-Ali et al., 2007). These methods offer improved stability in complex geology compared to ray-based ones (Sava and Biondo, 2004), and may also provide better resolution by taking advantage of the different information at different frequencies. The one-way wave equation-based MVA formulation is independent of the choice of propagator and data organization (Shen et al, 2003; Biondi and Sava, 2004; Khoury et al, 2006; Sava and Vlad, 2008). However, while shot-profile migration is now routine for depth imaging, the iterative nature of MVA makes a 3D shot-profile based inversion tremendously computationally intensive. On the other hand, CAM (Biondi and Palacharla, 1996), while potentially of limited applicability because of its assumptions, offers a very quick wave-equation based migration. For areas of moderate geological complexity, CAM provides as accurate an image as shot profile migration, but much more economically. So CAM provides an attractive framework for wave-equation based MVA. Khoury et al., 2006, presented a 2D DSR-based MVA tool in which the wave equation propagator is a GSP implemented in the mid-point offset domain. Hua et al., 2007, proposed a modified CAM, implementing the ffd wide-angle term in the source-geophone domain, which provides much better images in complex areas.

In this paper, we present a 3D implementation of DSO-based MVA based on the CAM of Hua et al, 2007; the adjoint state method is used to calculate the velocity gradient. The method is applied to 3-D synthetic and field data, validating the feasibility of the algorithm.

Theory

In this part, we briefly review the theory of FFD source geophone implementation of CAM, DSO principle, and adjoint state method.

The FFD source-geophone implementation of CAM was proposed by Hua, et al 2007. The common-azimuth DSR dispersion relation can be written as (Biondi and Palacharla, 1996):

$$Kz \approx Kz_x + \sqrt{\frac{4\omega^2}{v^2} - Km_y} - \frac{2\omega}{v_m} \qquad (1)$$

where

$$Kz_x = \sqrt{\frac{\omega^2}{v_s^2} - \frac{1}{4}(Km_x - Kh_x)^2} + \sqrt{\frac{\omega^2}{v_g^2} - \frac{1}{4}(Km_x + Kh_x)^2} \qquad (2)$$

equation (1) amounts to a 2-D inline prestack depth migration using equation (2), followed by a 2-D crossline poststack migration. The wide-angle term in the mid-point offset implementation of CAM uses the standard Padé approximation for the square roots in equation (2), but discards the relatively computationally expensive operator arising from the cross-term between Km_x and Kh_x. However, Kz_x can also be written as:

$$Kz_x = \sqrt{\frac{\omega^2}{v_s^2} - Ks_x^2} + \sqrt{\frac{\omega^2}{v_g^2} - Kg_x^2} \qquad (3)$$

The Padé approximation for the square roots in equation (3) gives operators which can be applied directly by effectively reorganizing the wavefield from mid-point-offset to source-geophone coordinates. This implicitly includes the previously-discarded cross-term, which is important for strong lateral velocity variation and high dips. We therefore expect, and numerical examples confirm, that the latter implementation delivers significantly better imaging in complex media, with no increase in cost. We therefore use this algorithm as the migration engine of our MVA method.

DSO was originally proposed by Symes and Carazzone, (1991). The basic idea is that when the velocity is correct, the normalized difference between neighbouring traces in a (angle) gather should be minimal. Subsequent work by Symes and co-authors has shown that the objective function is typically "well-behaved", with no secondary minima, over a large region of model space around the global minimum (Symes, pers.comm). As a result, various authors had developed inversion algorithm based on DSO (Shen et al, 2003, Chauris and Noble, 2001, Plessix et al, 2000). Shen and Calandra (2005) showed that the difference operator in a gather parameterized by reflection angle was equivalent to a multiplication by the subsurface offset and therefore proposed an MVA objective function of the form:

$$J = \left\| hI(X,h) \right\|^2 - \alpha \left\| I(X,0) \right\|^2 \qquad (4)$$

where α is the weight of the imaging power (second term) relative to the DSO objective function. X is the position vector (x,y,z), and h the subsurface offset.

The gradient of equation (4) is

$$J_c = \left(\frac{\partial I(X,h)}{\partial c} \right)^* h^2 I(X,h) - \alpha \left(\frac{\partial I(X,0)}{\partial c} \right)^* I(X,0) \quad (5)$$

We use the adjoint state method to calculate this gradient (cf. Shen et al, 2003, and Khoury et al, 2006) and either the L-BFGS method (Nocedal and Wright, 2000) or the steepest descent method can be used to drive the minimisation of the objective function

Synthetic Example

We first test our 3D MVA algorithm on the SEG/EAGE overthrust model. The model dimensions are 16km in the inline direction by 4km crossline. The simulated acquisition geometry is rather sparse, with a shot spacing of 200m in both inline and crossline directions, for a total of 1440 shots. Each shot is recorded by 11 streamers with 81 receivers each, with 40 meters spacing between streamers and receivers. The shot gathers were then regularized into common-azimuth data. The initial velocity model is a simple (1D) vertical gradient (Figures 1a, 2a). CAMVA was used to iteratively update the velocity model. The inverted region is 14km by 4km in inline and crossline directions, and 3km in depth. 450 cores were used and each iteration takes about 2 hours.

Figure 1 and 2 show representative slices from the initial, updated and true velocity models. Despite the simplicity of the initial velocity model, the sparsity of the acquisition and the limitations of the CAM method, the MVA did a good job to recover the low velocity block at shallow and high velocity block at deeper part. Figures 3 and 4 compare migrated images using the initial and updated velocity models, (due to space limitations, we do not show the corresponding images using the true velocity model). The image from the updated model is much better focused and more continuous. Figures 5 compares subsurface offset gathers using the initial and updated velocity models, showing a considerable improvement in the focusing in the latter case.

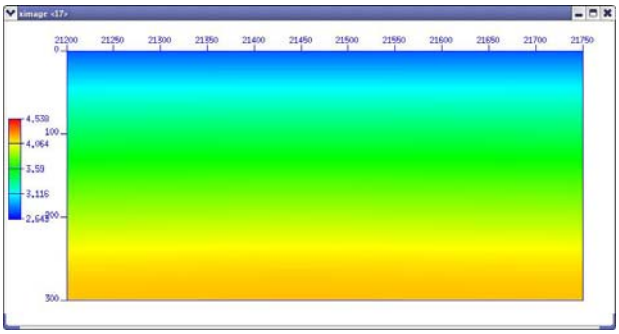

Figure 1a: Initial velocity model crossline slice

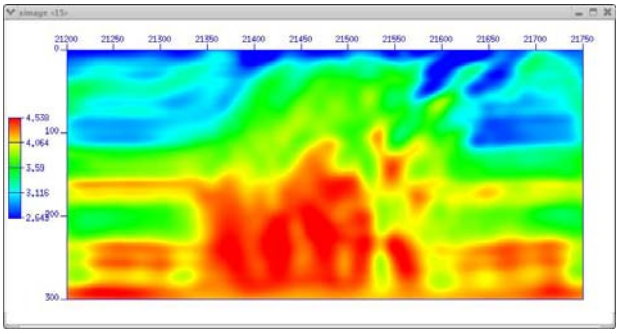

Figure 1b: Updated velocity model crossline slice

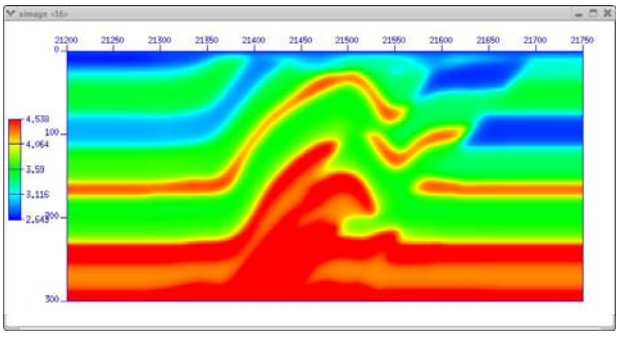

Figure 1c. True velocity model crossline slice

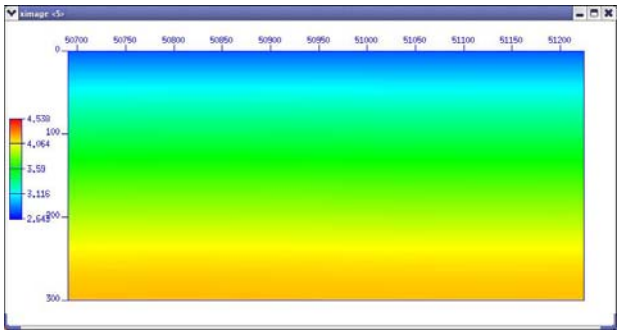

Figure 2a: Initial velocity model crossline slice

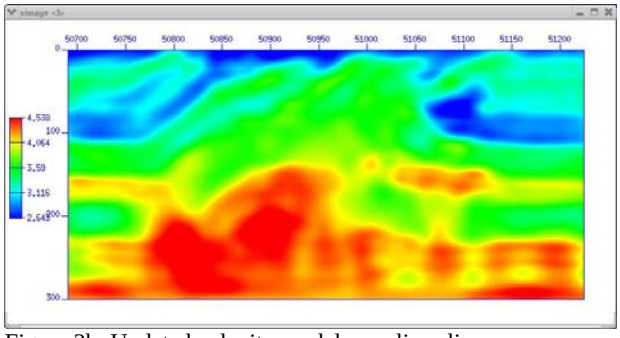

Figure 2b: Updated velocity model crossline slice

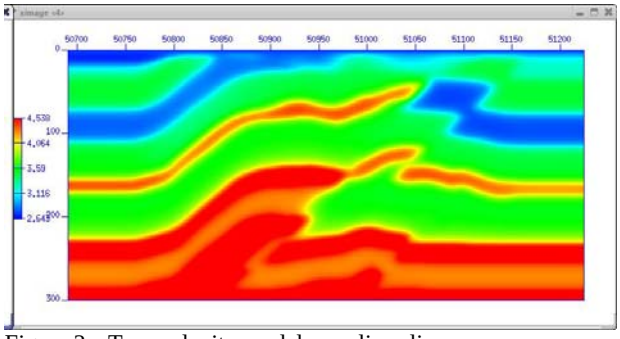

Figure 2c. True velocity model crossline slice

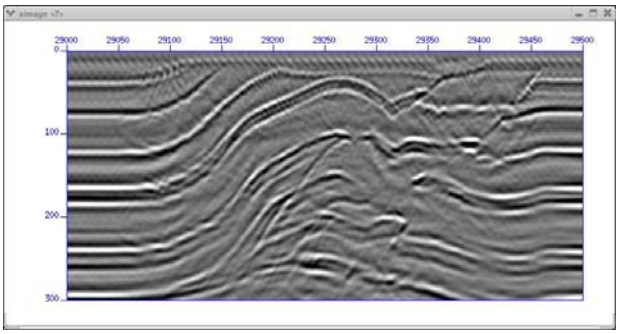

Figure 3a: Image slice using initial velocity model

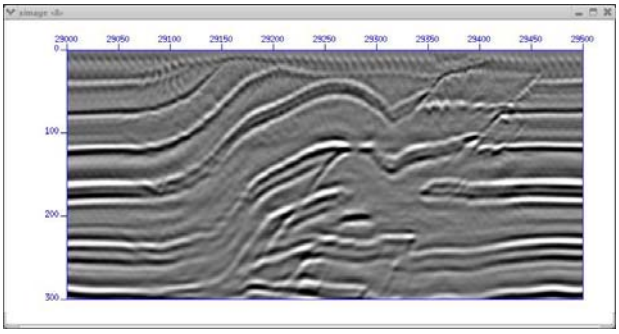

Figure 3b: Image using the updated velocity model

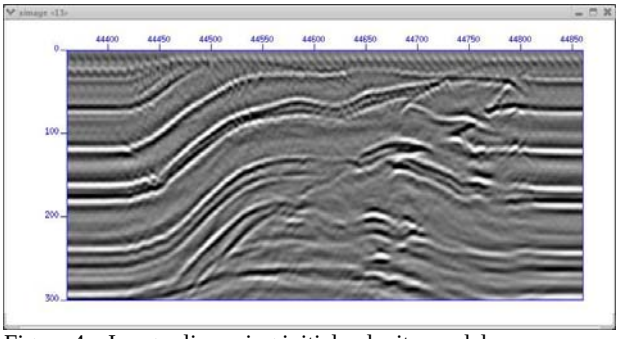

Figure 4a: Image slice using initial velocity model

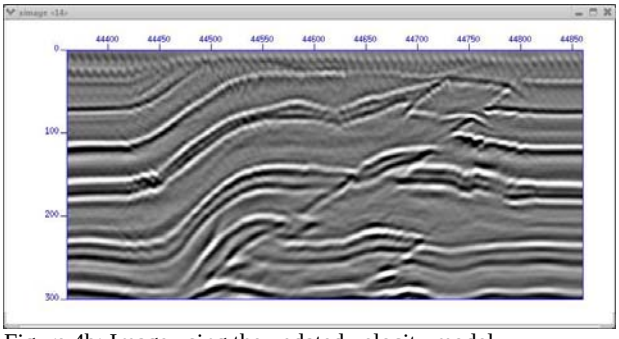

Figure 4b: Image using the updated velocity model

Field Example

We have also applied our MVA to a small real dataset from offshore Nigeria. The data volume is 17km inline by 5km crossline. Our initial velocity model was a simple vertical gradient below the water bottom (Figure 6a). The updated velocity model is shown in Figure 6b. A corresponding section is shown in figures 7a and 7b. We observe that the updated image (and gathers) show improved focusing, particularly in the central region. However we suspect that improvements are limited by the influence of anisotropy, which was not accounted for in this run and is the subject of ongoing research and development.

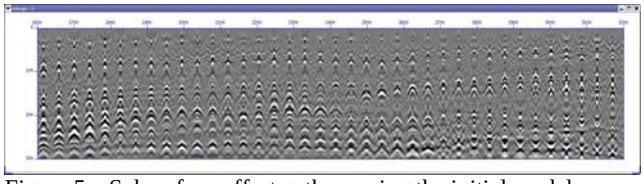

Figure 5a: Subsurface offset gathers using the initial model

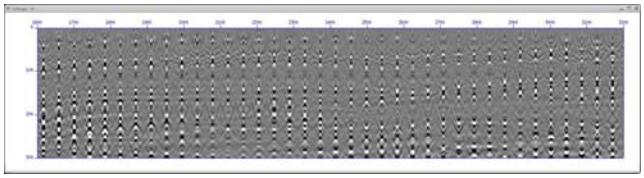

Figure 5b: Corresponding gathers using the updated model

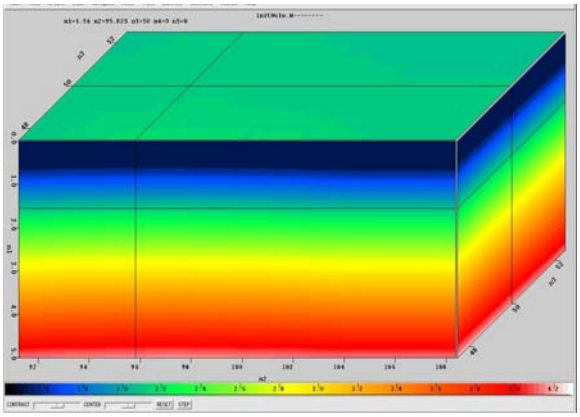

Figure 6a: initial 1-D velocity model for the field data

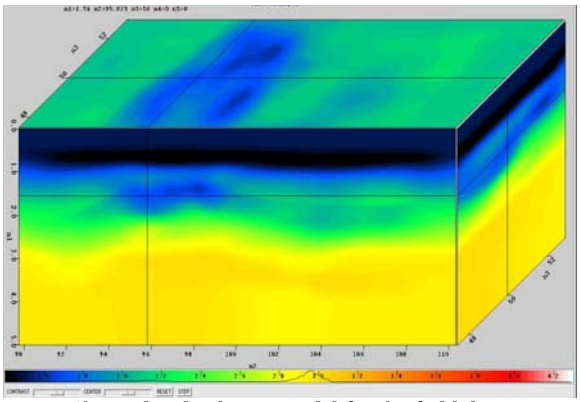

Figure 6b: Updated velocity model for the field data case

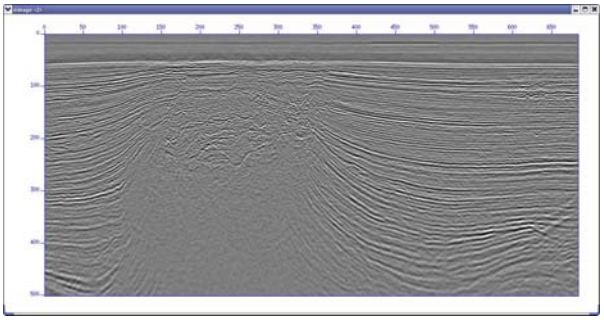

Figure 7a: Image using the initial velocity model

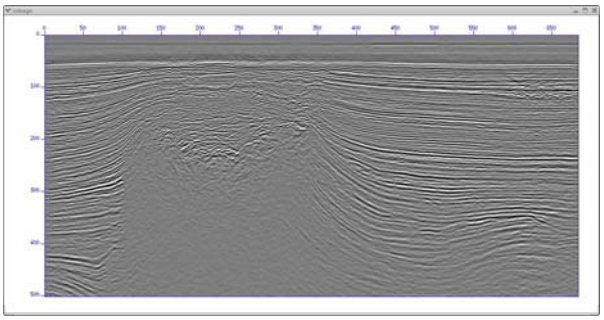

Figure 7b: Image using the updated velocity model

Conclusions

We have implemented a MVA tool in three dimensions, using the one-way wave-equation for forward and inverse propagation, and a reformulation of DSO in subsurface offset space for the inversion. The computational challenge is made feasible by applying the common-azimuth approximation to the DSR formulation of one-way wave-equation migration. The application of the wide-angle part of the FFD operator in source-geophone coordinates helps maintain the required accuracy when the common-azimuth assumption holds. Initial applications of the tool to 3D synthetic and field data examples gave good results, although ongoing upgrades to the tool should enable further improvements in due course. In both cases the inversion converged from a very simple initial model, which tends to confirm the theoretical robustness of DSO. While the tool can be used to estimate a velocity model from scratch, it can also be used to fine-tune an existing velocity model derived from, for example, ray-based tomography.

Acknowledgements

We thank Total E&P USA, Total E&P Nigeria Ltd., and Total SA for allowing the publication of this paper, and Professor W.W. Symes for many fruitful and illuminating discussions.

EDITED REFERENCES

Note: This reference list is a copy-edited version of the reference list submitted by the author. Reference lists for the 2009 SEG Technical Program Expanded Abstracts have been copy edited so that references provided with the online metadata for each paper will achieve a high degree of linking to cited sources that appear on the Web.

REFERENCES

Albertin, U., P. Sava, J. Etgen, and M. Maharramov, 2006, Adjoint wave-equation velocity analysis: 76th Annual International Meeting, SEG, Expanded Abstracts, 3345–3349.

Ben Hadj-Ali, H., S. Operto, J. Virieux, and F. Sourbier, 2007, 3D acoustic frequency-domain full-waveform inversion: 77th Annual International Meeting, SEG, Expanded Abstracts, 1730–1734.

Biondi, B., and G. Palacharla, 1996, 3-d prestack migration of common-azimuth data: Geophysics, **61**, 1822–1832.

Biondi, B., and P. Sava, 2004, Wave-equation migration velocity analysis I: Theory: Geophysical Prospecting, **52**, 593–623.

Bishop, T. N., K. Bube, R. Cutler, R. Langan, P. Love, J. Resnick, R. Shuey, D. Spindler, and H. Wyld, 1985, Tomographic determination of velocity and depth in laterally varying media: Geophysics, **50**, 903–923.

Chauris, H., and M. Noble, 2001, Two-dimensional velocity macro model estimation from seismic reflection data by local differential semblance optimization: Application synthetic and real data sets: Geophysical Journal International, **144**, 14–26.

Fliedner, M., M. Brown, D. Bevc, and B. Biondi, 2007, Wavepath tomography for subsalt velocity-model building: 77th Annual International Meeting, SEG, Expanded Abstracts, 1938–1942.

Khoury, A.,W. W. Symes, P. Williamson, and P. Shen, 2006, DSR Migration velocity analysis by differential semblance optimization: 76th Annual International Meeting, SEG, Expanded Abstracts, 2450–2454.

Nocedal, J., and S. Wright, 2000, Numerical optimization: Spring Verlag.

Plessix, R., F. ten Kroode, and W. Mulder, 2000, Automatic crosswell tomography by differential semblance optimization, 70th Annual International Meeting, SEG, Expanded Abstracts, 2265–2269.

Pratt, R. G., 1999, Seismic waveform inversion in the frequency domain, Part 1: Theory and verification in physical scale model: Geophysics, **64**, 888–901.

Sava, P., and I. Vlad, 2008, Numerical implementation of wave-equation migration velocity analysis operators: Geophysics, **73**, no. 5, VE145–VE159.

Sexton, P., and P. Williamson, 1998, 3D anisotropic velocity estimation by model-based inversion of pre-stack traveltimes: 68th Annual International Meeting, SEG, Expanded Abstracts, 1855–1858.

Shen, P., and H. Calandra, 2005, One-way waveform inversion within the framework of adjoint state differential migration: 75th Annual International Meeting, SEG, Expanded Abstracts, 1709–1712.

Shen, P., W. Symes, and C. Stolk, 2003, Differential semblance velocity analysis by wave-equation migration: 73th Annual International Meeting, SEG, Expanded Abstracts, 2135–2139.

Symes, W., and J. Carazzone, 1991, Velocity inversion by differential semblance optimization: Geophysics, **56**, 654–663.

Tarantola, A., 1984, Inversion of seismic reflection data in the acoustic approximation: Geophysics, **49**, 1259–1266.

Xie, X., and H. Yang, 2008, A wave-equation migration velocity analysis approach based on the finite-frequency sensitivity kernel: 78th Annual International Meeting, SEG, Expanded Abstracts, 3093–3097.